www.czasopisma.pan.pl PAN POLSKA AKADEMIA NAUK www.journals.pan.pl

Arch. Metall. Mater. **68** (2023), 4, 1525-1531

DOI: https://doi.org/10.24425/amm.2023.146219

LINGEN LUO[1], JIANMING PANG[1]*, YAOXIN SONG[1], SHULAN LIU[2]*, GUOLIANG YIN[3], HAO PENG[4], CHUNLEI PU[5], YINHE LIN[4], JINGWEI LI[6], XUEFENG SHI[7]

MICROSTRUCTURE EVOLUTION MECHANISM OF AISI 1045 STEEL UNDER HIGH SPEED DEFORMATION

AISI 1045 steel has the characteristics of high strain rate, large strain, and sharp rise in temperature during high-speed deformation process, resulting in a concentrated deformation band and fine structure. In this work, the microstructure of submicron-sized grains in AISI 1045 steel material formed under 10^6 s^{-1} during a high speed cutting process was examined. To reveal the dynamic evolution mechanism of the AISI 1045 microstructure, the continuous dynamic recrystallization theory was introduced. The results show a high dislocation density which favor the formation of small angle grain boundaries during the high speed cutting process. Kinetics calculations that use continuous dynamic recrystallization mechanisms prove that the recrystallization size is constant when the strain rate increases from 10^3 s^{-1} to 10^6 s^{-1}, and the transition time is reduced from 6×10^{-5} s to 4×10^{-8} s. The recrystallization grains were gradually formed during the deformation of the material, not generated after the deformation.

Keywords: High speed cutting; Continue dynamic recrystallization; Microstructure evolution; Microstructure; AISI 1045 steel

1. Introduction

When metallic materials are subjected to extreme deformation loads characterized by high deformation speed and large strain, they usually undergo macroscopic localization of the deformation, form a concentrated shear zone, and result in plastic instability [1-3]. In earlier research on metal material microstructures, the bright white high-hardness bands in the concentrated deformation zone assumed to be martensitic products formed via phase transformation [4-6]. Later on, transmission electron microscopy, field emission scanning electron microscopy, and electron back-scattered diffraction (EBSD) were applied to investigate the microstructure, and the results proved that equiaxed non-distortion crystal grains of sub-micron size were formed in the concentrated deformation zone [7,8].

The mechanism of sub-micron recrystallized grains in the concentrated shear zone is of great significance for elucidating the recrystallization softening model under extremely high strain rate deformation [9,10]. To explain the dynamic recrystallization phenomenon in high-speed deformation, Pere-Prado et al. [1] proposed a model in which an external stress is applied to the gradual rotation of the crystal grains for realizing the dynamic recrystallization. However, the mechanical rotation of crystal grains in the model does not consider the problem of cracks caused by the coordinated deformation of grains with neighboring grains [11]. Nesterenko et al. also proposed a dynamic recrystallization model based on rotation [6]. The metal material has a bamboo-like elongated deformation substructure under high-speed deformation and large strain [12,13], and the boundary of the orientation angle with the lowest boundary energy can be diffused to transform the deformed substructure into dynamic recrystallized grains with equiaxed microscopic orientation angles [14]. However, this process requires the matrix atoms to diffuse from the original boundary to a nearby location and form a new grain boundary, which is difficult to achieve in the view of material dynamics [15].

The deformation of metals during cutting is a process that typically has a high strain rate ($\geq10^3$ s^{-1}) and large strain (≥1 s^{-1}) [16-18]. This paper aims to study the evolution mechanism of dynamic recrystallization microstructure of metal materials under very high rate, large strain and sudden temperature rise deformation. In the present paper, the influence of large,

[1] RESOURCE APPLICATION AND ALLOY MATERIALS DIVISION, CHINA IRON AND STEEL RESEARCH INSTITUTE GROUP, BEIJING, 100081, P.R. CHINA
[2] TANGSHAN NORMAL UNIVERSITY, SCHOOL OF PHYSICAL SCIENCE AND TECHNOLOGY, TANGSHAN, 063000, P.R. CHINA
[3] YIBIN UNIVERSITY, DEPARTMENT OF MATERIALS AND CHEMICAL ENGINEERING, YIBIN, 644000, P.R. CHINA
[4] YANGTZE NORMAL UNIVERSITY, INSTITUTE OF CHEMICAL ENGINEERING, CHONGQING, 408100, P.R. CHINA
[5] MCC HUATIAN ENGINEERING & TECHNOLOGY CORPORATION, NANJING, 210019, P.R. CHINA
[6] SCHOOL OF MATERIALS SCIENCE AND ENGINEERING, HEFEI UNIVERSITY OF TECHNOLOGY, HEFEI, 230009, P.R. CHINA
[7] NORTH CHINA UNIVERSITY OF SCIENCE AND TECHNOLOGY, COLLEGE OF METALLURGY AND ENERGY, TANGSHAN, 063210, P.R. CHINA

* Corresponding authors: pangjianming198012@163.com, shulan070@126.com

high-speed deformation on microstructure was investigated by high speed cutting experiment. Then, the Continuous dynamic recrystallization mechanism (CDRM) under high deformation speed was studied. Finally, the dynamic model of the evolution of large, microscopic orientation angles based on CDRM at high deformation speeds was analyzed.

2. Materials and methods

Industrially produced normalized steel AISI 1045 (hardness is 242 HB) with the composition shown in TABLE 1 is used as the workpiece material. An orthogonal turning experiment was conducted, and the workpiece was processed into a hollow cylindrical sample with an outer diameter of 150 mm, inner diameter of 110 mm, and a length of 500 mm. The cutting tool is made of uncoated cemented carbide with a cobalt content of 8%, and the hardness is 607 HB. The rake angle of the cutting tool is 0°, and the back angle in the holder is 7°. The cutting edge radius is approximately 0.5 mm. In order to evaluate the high-speed deformation of the material, the cutting analysis model for deformation parameters (like strain rate, strain, and temperature) was applied by Oxley et al. [16,19,20]. The cutting speed specified in the experiment is 560 m/min (corresponding to the root strain rate of the chip is about 10^6 s^{-1}, the strain is about 5, and the temperature is 950°C), and the feed and cutting width are 0.1 mm/min and 2 mm respectively. The cutting time is 30 s. After the orthogonal cutting experiment, the chips were collected. The macrostructure and microstructure of the chips were observed by optical microscope and field emission scanning electron microscope.

TABLE 1

Chemical composition of test steel AISI 1045 (mass fraction, %)

C	Si	Mn	P	S	Cr	Ni	Mo
0.43	0.26	0.68	0.01	0.03	0.15	0.1	0.02

3. Results and discussion

3.1. Influence of large, high-speed deformation on microstructure

The experimentally obtained microscopic and macroscopic morphology of the chip and the electronic scanning detection map of the concentrated deformation area in the AISI 1045 steel at a cutting speed of 560 m/min are shown in Fig. 1.

Fig. 1(a) shows the macroscopic metallographic morphology of the chip. Fig. 1(b) shows the macroscopic metallography of the root deformation zone, and Fig. 1(c) shows the scanning electron microscope image of the root deformation zone when the cutting speed is 560 m/min. As can be seen from Fig. 1(a), the overall deformation of the material is non-uniform. Particularly, the root of the chip material has obvious deformation and concentration, and a bright white band appears in Fig. 1(b). In addition, some fine structures are observed in Fig. 1(c). Because the deformation and distortion in the shear zone are serious and small, the characterization of the formed microstructure size is very difficult [8]. Courbon et al. applied EBSD to observe the shear zone in the AISI 1045 steel chip (Fig. 2(a)) with lower cutting speed compared to this study and confirmed that the structure has grains [8]. However, due to the high degree of distortion

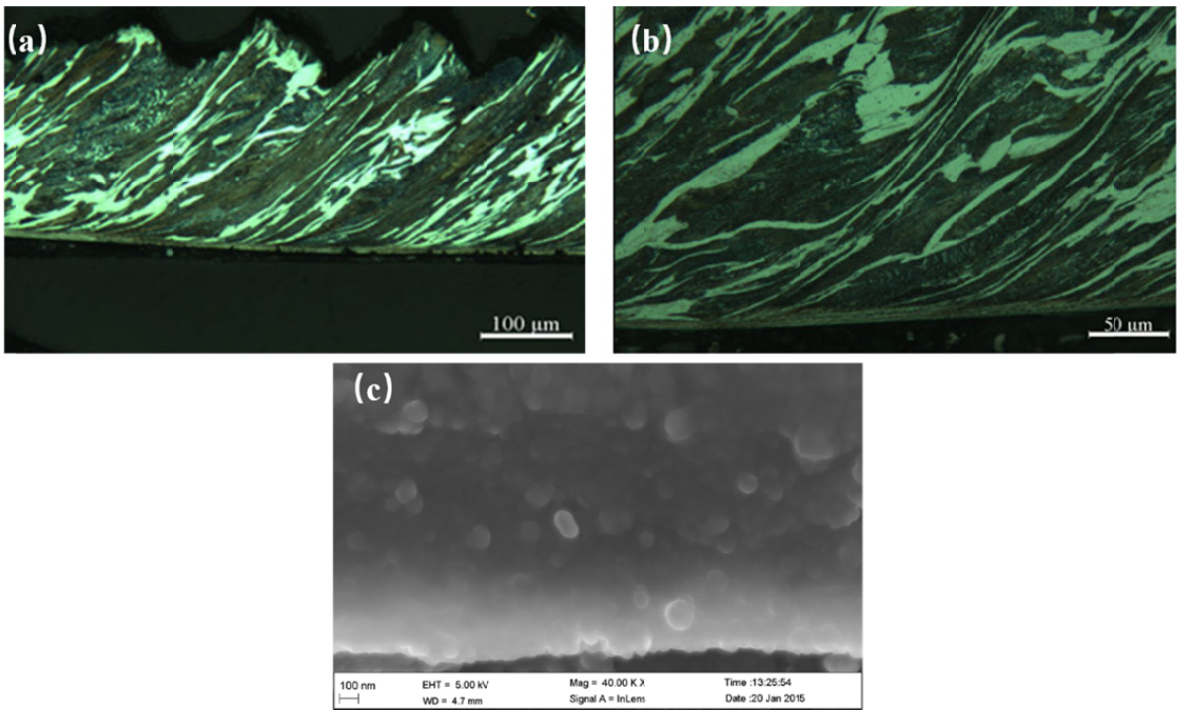

Fig. 1. Chip morphology and microstructure of second deformation zone of AISI 1045 steel at a cutting speed of 560 m/min (a) Chip macromorphology, (b) Metallographic morphology of chip root, (c) Chip root microstructure by SEM

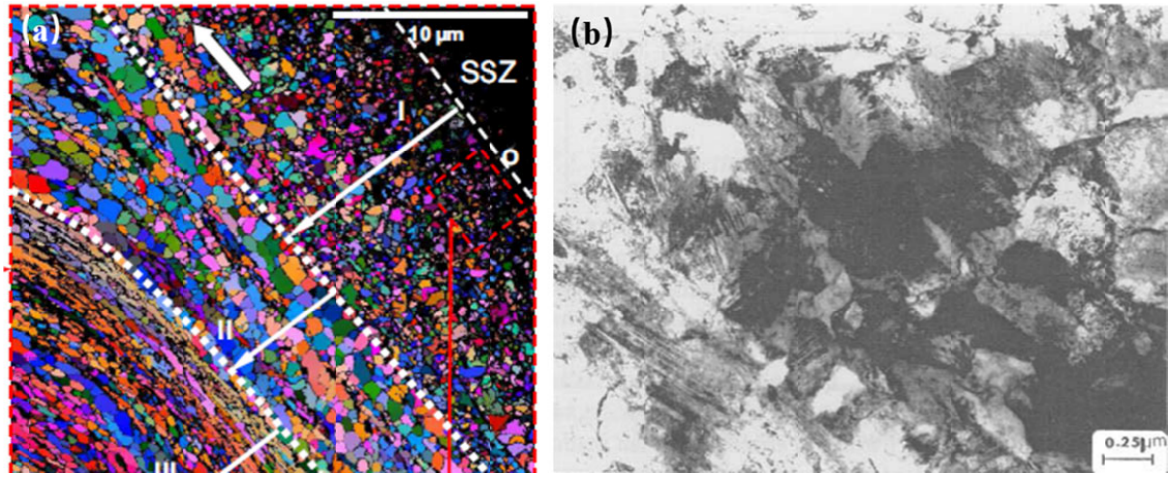

Fig. 2. Microstructure inspection of second shear zone of the chips during high-speed cutting of AISI 1045 steel (a) Chip root microstructure detected by EBSD [8], (b) Chip root microstructure detected by TEM [10]

in the deformation zone, blind spots (black areas in the figure) appeared in the near-root zone of the sample, and only minimal fine structures were observed [21]. Through high-resolution projection electron microscopy, Subramanian et al. observed dynamic recrystallized grains of 0.25 μm size in the shear zone of the AISI 1045 steel chip roots (Fig. 2(b)) [10].

3.2. Continuous dynamic recrystallization mechanism (CDRM) under high deformation speed

During high-speed deformation, materials deform at a high strain rate and are subjected to stress only for a short time. The recrystallized grain size becomes larger based on polygonization and sub-grain merging to form large-angle grain boundaries. The bow of the angle grain boundary becomes larger.

The continuous dynamic recrystallization mechanism points out that the dislocation configuration in the material forms a dislocation cell structure. The density of dislocations in the cell structure increased with the increase in deformation. The dislocations inside the cell accumulate towards the cell wall. The misorientation of the sub-cells increases, and finally sub-crystals with large-angle grain boundaries are formed, thus completing the recrystallization process. In this mechanism, dislocation motions such as dipole cancellation, polygonization, and sub-crystal merging act to release strain energy and complete the recrystallization process. There is no long-range diffusion of atoms, and it may be exist in high-speed deformation.

Theoretically, the flow stress of a material is proportional to the square root of the dislocation density in the material, namely [22]:

$$\sigma = \alpha \mu b \sqrt{\rho} \tag{1}$$

Among them, a is the material constant, μ is the shear modulus, and b is the Burgers vector.

In high-speed deformation, the strain rate is very high, and the flow stress increases under the same strain condition. Therefore, the large strains under high-speed conditions will not only increase the speed of dislocation movement, but also activate more dislocation sources.

To decrease their configuration energy, the dislocations generate dislocation entanglement and form dislocation cell structure. Therefore, it can be considered that the effect of strain rate hardening under high-speed deformation conditions will have a higher dislocation density than under normal strain conditions, resulting in more dislocation cell structures. At the same time, high strain rate and large strain will increase the temperature and provide dynamic conditions for dislocation climbing and polygonalization, which is beneficial to the formation of the dislocation cell structure. The higher the high-speed deformation rate, the greater the deformation rate, and the smaller the cell structure. Because of the accumulation of dislocations in the cell wall, the difference in the orientation of the sub-cells on both sides of the thin wall will increase. The high dislocation density and speed of dislocation movement will facilitate the formation and refinement of the sub-crystal size.

Obviously, the formation of continuous recrystallized sub-crystals mainly involves dislocation movement and changes in the dislocation configuration. Here, time is a critical factor. Therefore, the continuous dynamic recrystallization mechanism should be investigated for the formation of fine recrystallized grains during high-speed deformation. This can be analyzed from the time required for the formation of sub-crystals during the deformation process.

3.3. Dynamic model of the evolution of large, microscopic orientation angles based on CDRM at high deformation speeds

In the continuous dynamic recrystallization process, the main factor that affects the recrystallization kinetics is the time when the dislocation cellular structure forms sub-grains with large angle grain boundaries [23]. The sub-cells with small

TABLE 2

Main parameters in the calculation of continuous dynamic recrystallization kinetics of ferritic steel [22,28]

	D	a	v	μ	ρ_0	b	q_0	δ	H	M	t_s
Unit	μm			GPa	m^{-2}	m	°	nm	MPa	m^{-2}	MPa
Value	0.2	0.75	0.32	80	1×10^{10}	2.94×10^{-10}	5	5 nm	750	5×10^{14}	1400

angle micro-orientation angle interface (generally considered at 5°C) formed in the deformation process, based on the internal dislocation, gradually moves to the cell wall [24-26]. The time required to transform the cell wall into a large-angle micro-orientation interface is generally considered at 15°C [27,28]. For dislocation cells with small angle micro- orientation angle, the average dislocation cell wall energy per unit length η is given by [29,30]:

$$\eta = \alpha\mu b\theta\left(1-\frac{\ln(\theta)}{4\pi(1-\nu)\alpha}\right) \tag{2}$$

Among them, α is the material constant (0.5~1), μ is the shear modulus, b is Burgers vector, θ is dislocation cell microscopic orientation angle, and v is Poisson's ratio.

If the dislocation cell diameter is D and the dislocation cell wall thickness is δ, then the dislocation cell wall energy can be constructed from two aspects: microscopic orientation angle and dislocation density within the dislocation cell wall [25]:

$$\frac{d}{dt}\left[hp\left(\frac{D}{2}\right)^2\right] = amb^2 p\left(\frac{D}{2}\right)^2 d\frac{d\rho_w}{dt} \tag{3}$$

Among them, ρ_w is the average dislocation density in the dislocation cell wall.

The change in dislocation density in the dislocation cell wall in unit time $\frac{d\rho_w}{dt}$ is related to the mobile dislocation density in the dislocation cell (ρ_m) and strain in unit time [28]:

$$\frac{d\rho_w}{dt} = \left(\frac{2}{3}\right)^{1/2}\left(\frac{D}{db}\right)\rho_m^{1/2}\frac{de}{dt} \tag{4}$$

$$\rho_m = (\rho_0 + Me)\exp\left(-\frac{He}{t_S}\right) \tag{5}$$

Among them, ρ_0 is the initial dislocation density, M is the dislocation plug product coefficient, H is the hardening coefficient, and t_s is the shear stress of loading.

In this work, continuous dynamic recrystallized mechanism, and changes under micro-orientation angle of interface with small angle, to the large angle micro orientation angle of interface were investigated, which would require $\theta(t)$ *as* the function relation, so supposing dislocation cell size D was kept constant, simultaneous Eq. (4)~(5) after reduction get dislocation cell micro differential relationship between expression of orientation angle varies with time t [29]:

$$\frac{dq}{dt} = \frac{4p(1-n)aD}{\left[4p(1-n)a-1-\ln(q)\right]}\sqrt{\frac{2}{3}\left(\rho_0 + M\frac{\dot{e}t}{\sqrt{3}}\right)}\exp\left(-\frac{H\dot{e}t}{2\sqrt{3}t_S}\right)\frac{\dot{e}}{\sqrt{3}} \tag{6}$$

As can be seen from equation (6), the relation $\frac{d\theta}{dt}$ is complex and it is difficult to obtain the functional relation $q(t)$ analytically. Therefore, numerical integration is performed on Eq. (6) to obtain the microscopic orientation angle over time. The parameters in the calculation of steel grades are shown in TABLE 2, and the obtained calculation result is shown in Fig. 3.

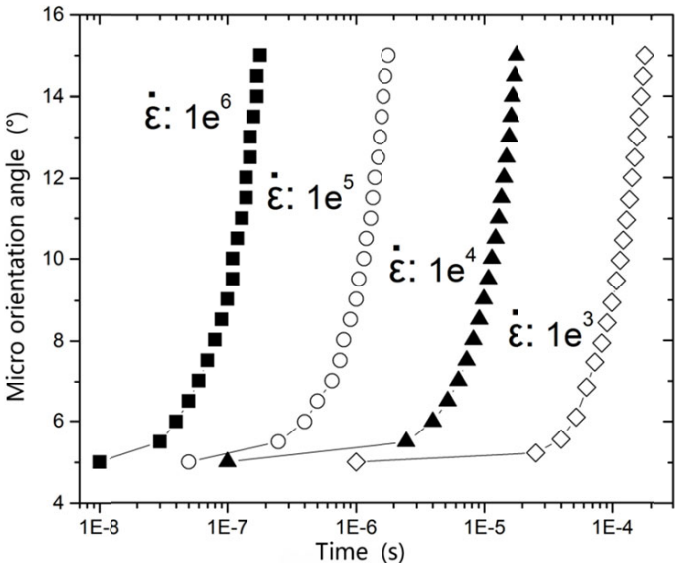

Fig. 3. Evolution of micro-orientation angle under different strain rates based on continuous dynamic recrystallization mechanism

Fig. 3 shows the evolution of micro-orientation angle under different strain rates based on continuous dynamic recrystallization mechanism. The dislocation entanglement and micro orientation angle follow a similar pattern the increase in deformation time. Initially, the micro orientation angle increases slowly, and then rises sharply, until it suddenly the critical micro orientation angle values q_c (15°) of the small angle interface and large angle interface. The process time is very short, and the strain rate is 10^3, with the change in the order of magnitude of the time required controlled to 6×10^{-5} s. The transition time decreases significantly with increasing strain rate and for a 10^6 s^{-1} strain rate, the time is as low as 4×10^{-8} s. Based on continuous dynamic

recrystallization mechanism, the deformation time was halved during the high speed cutting process [31].

Meanwhile, because of the large angle interface and large migration capacity, the grains formed during dynamic recrystallization becomes larger after the deformation of materials [32].

According to theory of Hines [1] and Meyer et al. [6], the grain with a radius S migrated towards the deformation matrix from the boundary by atomic diffusion when the temperature is T. The time t required for the grain size to reach L can be calculated by the following formula [1,6]:

$$t(T) = \frac{SLkT}{6\delta b^2 \mu\theta D_0 \exp(-Q/RT)} \tag{7}$$

Among them, k is the Boltzmann constant (1.38×10^{-23} J/K), D_0 is the grain boundary diffusion coefficient (13.0×10^{-5} m^2/s), Q is grain boundary diffusion activation energy (167000 J/mol), and other parameter values are shown in TABLE 2.

According to Oxley et al. [16], the dynamic recrystallization grain size obtained by the chips at high speed cutting deformation rate is generally in the submicron level. Taking 0.5 μm as the grain size, Eq. (7) can be used to compute the value under different temperatures (300°C~1400°C). The grain size increases from 0.1 μm to 0.5 μm, and the results are shown in Fig. 4.

As can be seen from Fig. 4, temperature has a decisive influence on the time required for grain boundaries to reach a certain size. At 1400°C, 0.5 μm recrystallization grains require 10^{-3} s, 0.5×10^{-3} s, and 10^{-2} s to grow 0.1 μm, 0.25 μm, and 0.5 μm respectively. With the decrease in temperature, the time required for grain growth increases significantly. Especially at 800°C, the time required for grain growth is approximately 10^2 s. When cutting speed was 560 m/min, and the highest chip interface temperature was 950°C, the time required for 0.1 μm growth was approximately 5 s, but the corresponding strain rate in the deformation zone was approximately 10^6, the strain exceeded 5, and the deformation time was approximately 5×10^{-6} s. Therefore, the recrystallization grains were formed gradually during the deformation of the material, and not generated after the deformation.

Fig. 5 shows the dynamic recrystallization process of CDRX under high strain rate deformation: (a) A large number of dislocations are formed under extremely high-strain-rate deformation; (b) The movement of micro-dislocations is faithful, and the dislocation cells are formed by entanglement; (c) High strain rate and large deformation coupled with hardening lead to high flow stress and high temperature rise of plastic deformation, which increases the temperature of the deformation zone above 0.3 Tm; the displacement ability of the dislocation is enhanced, enlarging the small angle grain boundary from θ1 to θ2.

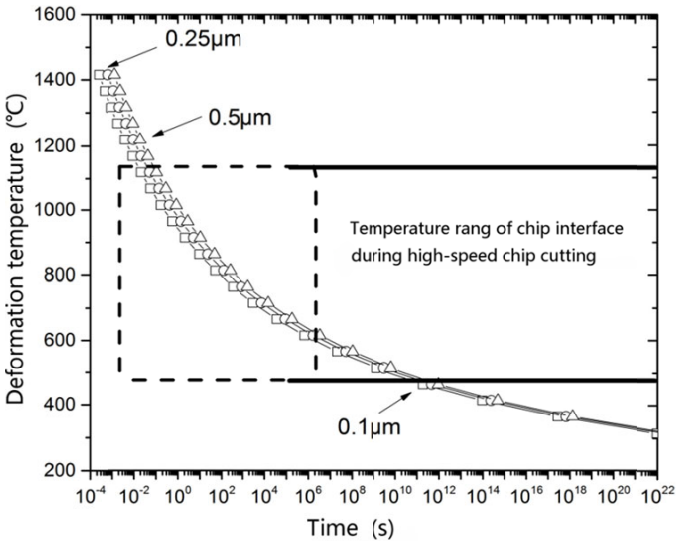

Fig. 4. Relationship between time and deformation temperature

4. Conclusion

(1) The second deformation zone sends concentrated shear deformation, the macroscopic metallography is white and bright, and the fine microstructure formed is dynamic recrystallization at the cutting rate of 560 m/min, strain rate of 10^6 s^{-1}, 950°C, and strain of 5.

(2) The high dislocation density causes the deformation microstructure to evolve rapidly to the substructure with the high dislocation density inside. The high deformation temperature provides the foundation for dislocation movement in the substructure to the substructure wall and the transformation from small angle boundary to large angle interface.

(3) This study shows that continuous dynamic recrystallization mechanism meets the characteristics of very short high-speed deformation time, and the time required for the transformation decreases from 6×10^{-5} s to 4×10^{-8} s when the strain rate changes from 10^3 to 10^6.

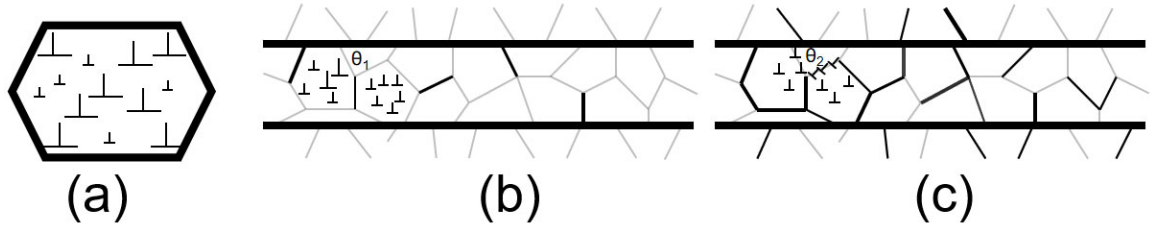

Fig. 5. Schematic representation of the CDRX microstructure under high speed deformation: (a) Initial deformation grains, (b) Lamellar structure with LAGBs and HAGBs at early stages of high-speed deformation formed by high density dislocations, (c) Transformation of LAGBs to HAGBs by the continuous increase in misorientation

5. Future research

In this paper, the continuous dynamic recrystallization mechanism is used to explain the evolution of the microstructure of materials under high-speed deformation, and the subsequent work will focus on the following aspects:

1) How the internal dislocation density evolved after dynamic recrystallization formation.
2) What is the criticality process parameters for microstructure evolution with increasing high speed deformation.
3) The impact of microstructure evolution on the follow stress and macroscopic morphology of chip serration at high speed cutting.

Acknowledgments

This research was supported by the Project of the National Natural Science Foundation of China (Grant No. U1960101, No.51874272 and No. 52111540265), Sichuan Science and Technology Program (No. 2021YJ0548), Chongqing Municipal Natural Science Foundation (cstc2020jcyj-msxmX0060), Panzhihua Science and Technology Project (Grant No. 2020CY-G-15), the Open Project of the State Key Laboratory of Advanced Metallurgy (KF20-03), Key Laboratory of Comprehensive Utilization of Vanadium and Titanium Resources in Sichuan Province (2019FTSZ06), the PhD Fund of Panzhihua University, and Funded by the State Key Laboratory of Vanadium and Titanium Resources Comprehensive Utilization; Open Foundation of State Key Laboratory of Mineral Processing (No. BGRIMM-KJSKL-2022-23) and Open Foundation of State Key Laboratory of Complex Nonferrous Metal Resources Clean Utilization (No. CNMRCUKF2205), Scientific Research Key Project of Yibin University (412-0219020202); The Education and Teaching Reform Project of Tangshan Normal University of China (Grant No. 2019JG020); Sichuan Vanadium and Titanium Industry Development Research Center(2020VTCY-Y-02); Sichuan Vanadium titanium Material Engineering Technology Research Center (2022FTGC06).

REFERENCES

[1] M.T. Perez-Prado, J.A. Hines, K.S. Vecchio, Microstructural evolution in adiabatic shear bands in Ta and Ta–W alloys, Acta Mater. **49** (15), 2905-2917 (2001).
DOI: https://doi.org/10.1016/S1359-6454(01)00215-4

[2] J.B. Li, J. Lu, C.Y. Chen, J.Y. Ma, X.P. Liao, Tool wear state prediction based on feature-based transfer learning, Int. J. Adv. Manuf. Tech. **113** (11/12), 3283-3301 (2021).
DOI: https://doi.org/10.1007/s00170-021-06780-6

[3] D. Zhang, X.M. Zhang, G.C. Nie, Z.Y. Yang, H. Ding, In situ imaging based thermo-mechanical analysis of built-up edge in cutting process, J. Manuf. Process. **71**, 450-460 (2021).
DOI: ,https://doi.org/10.1016/j.jmapro.2021.09.040

[4] D. Ambrosio, A.Tongne, V. Wagner, G. Dessein, O. Cahuc, A new damage evolution criterion for the coupled Eulerian-Lagrangian approach: Application to three-dimensional numerical simulation of segmented chip formation mechanisms in orthogonal cutting. J. Manuf. Process. **73**, 149-163 (2022).
DOI: https://doi.org/10.1016/j.jmapro.2021.10.062

[5] T.E.F. Silva, A.V.L. Gregório, A.M.P. de Jesus, P.A.R. Rosa, An Efficient Methodology towards Mechanical Characterization and Modelling of 18Ni300 AMed Steel in Extreme Loading and Temperature Conditions for Metal Cutting Applications, J. Manuf. Mater. Process. **5** (3), 83 (2021).
DOI: https://doi.org/10.3390/jmmp5030083

[6] V.F. Nesterenko, M.A. Meyers, J.C. LaSalvia, M.P. Bondar, Y.J. Chen, Y.L. Lukyanov, Shear localization and recrystallization in high-strain, high-strain-rate deformation of tantalum, Mater. Sci. Eng. A. **229** (1-2), 23-41 (1997).
DOI: https://doi.org/10.1016/S0921-5093(96)10847-9

[7] D. Zhang, X.M. Zhang, G.C. Nie, Z.Y. Yang, H. Ding, Characterization of material strain and thermal softening effects in the cutting process, Int. J. Mach. Tool. Manu. **160**, 103672 (2021).
DOI: https://doi.org/10.1016/j.ijmachtools.2020.103672

[8] C. Courbon, T. Mabrouki, J. Rech, D. Mazuyer, F. Perrard, E. D´Eramo, Further insight into the chip formation of ferritic-pearlitic steels: Microstructural evolutions and associated thermo-mechanical loadings, Int. J. Mach. Tool. Manu. **77**, 34-46 (2014).
DOI: https://doi.org/10.1016/j.ijmachtools.2013.10.010

[9] T. Zhou, L. He, Z.F. Zou, F.L. Du, J.X. Wu, P.F. Tian, Three-dimensional turning force prediction based on hybrid finite element and predictive machining theory considering edge radius and nose radius, J. Manuf. Process. **58**, 1304-1317 (2020).
DOI: https://doi.org/10.1016/j.jmapro.2020.09.034

[10] S.V. Subramanian, H.O. Gekonde, G. Zhu, X. Zhang, Role of microstructural softening events in metal cutting, Mach. Sci. Technol. **6** (3), 353-364 (2002).
DOI: https://doi.org/10.1081/mst-120016250

[11] M. Storchak, P. Rupp, H. Möhring, T. Stehle, Determination of Johnson-Cook Constitutive Parameters for Cutting Simulations, Metals **9** (4), 473 (2019).
DOI: https://doi.org/10.3390/met9040473

[12] M. Stojković, M. Madić, M. Trifunović, R. Turudija, Determining the Optimal Cutting Parameters for Required Productivity for the Case of Rough External Turning of AISI 1045 Steel with Minimal Energy Consumption, Metals **12**, 1793 (2022).
DOI: https://doi.org/10.3390/met12111793

[13] J. R. Xiao, Z. Zhao, X.C. Xie, Z.W. Liang, Z.Y. Liu, X.C. Liu, R.Z. Tang, Micromorphology, Microstructure, and Wear Behavior of AISI 1045 Steels Irregular Texture Fabricated by Ultrasonic Strengthening Grinding Process, Metals **12**, 1027 (2022).
DOI: https://doi.org/10.3390/met12061027

[14] Q. Lu, C. Zhang, W. Wang, S. Jiang, A. Lee, Y. Tabassam, J. Jiang, Reveal the Viscoplastic Behaviour and Microstructure Evolution of Stainless Steel 316L, Materials **15**, 7064 (2022).
DOI: https://doi.org/10.3390/ma15207064

[15] L. Wang, L.K. Ji, K. Yang, X.X. Gao, H.Y. Chen, Q. Chi, The Flow Stress-Strain and Dynamic Recrystallization Kinetics Behavior of High-Grade Pipeline Steels, Materials **15**, 7356 (2022).
DOI: https://doi.org/10.3390/ma15207356

[16] P.L.B. Oxley, Mechanics of Machining: an Analytical Approach to Assessing Machinability, England 1989.

[17] B. Medina-Clavijo, J. Rafael-Velayarce, E. Modin, M. Saez-de-Buruaga, D. Soler, C. Motz, P.J. Arrazola, A. Chuvilin, Mechanical properties of friction induced nanocrystalline pearlitic steel, Nature. **12**, 12591 (2022).
DOI: https://doi.org/10.21203/rs.3.rs-1332231/v1

[18] T. Morikawa, K. Higashida, T. Sato, Fine-grained structures developed along grain boundaries in a cold-rolled austenitic stainless steel, ISIJ Int. **42** (12), 1527-1533 (2022).
DOI: https://doi.org/10.2355/isijinternational.42.1527

[19] W. Cai, Y.Q. Li, L. Li, K.H. Lai, S. Jia, J. Xie, Y.H. Zhang, L.K. Hu, Energy saving and high efficiency production oriented forward-and-reverse multidirectional turning: Energy modeling and application, Energy **252**, 123981.1-12 (2022).
DOI: https://doi.org/10.1016/j.energy.2022.123981

[20] A. Awale, K. Inamdar, Multi-objective optimization of high-speed turning parameters for hardened AISI S7 tool steel using grey relational analysis, J. Braz. Soc. Mech. Sci. **42** (7), 1-17 (2020).
DOI: https://doi.org/10.1007/s40430-020-02433-z

[21] Z.Y. Yang, X.M. Zhang, G.C. Nie, D. Zhang, A comprehensive experiment-based approach to generate stress field and slip lines in cutting process, J. Manuf. Sci. Eng. **143** (7), 071014 (2021).
DOI: https://doi.org/10.1115/1.4049848

[22] Q.L. YONG, The Second Phase of Steel, Beijing 2006.

[23] C.J. Shi, W.M. Mao, X.G. Chen, Evolution of activation energy during hot deformation of AA7150 aluminum alloy, Mater. Sci. Eng. A. **571**, 83-91 (2013).
DOI: https://doi.org/10.1016/j.msea.2013.01.080

[24] S. Gourdet, F. Montheillet, A model of continuous dynamic recrystallization, Acta Mater. **51** (9), 2685-2699 (2003).
DOI: https://doi.org/10.1016/S1359-6454(03)00078-8

[25] X.L. Liang, Z.Q. Liu, B. Wang, Multi-pattern failure modes and wear mechanisms of WC-Co tools in dry turning Ti–6Al–4V, Ceram. Int. **46**, 24512-24525 (2020).
DOI: https://doi.org/10.1016/j.ceramint.2020.06.238

[26] U. Messerschmidt, Dislocation dynamics during plastic deformation, Germany 2010.

[27] H. Chouhad, Towards online metrology for proactive quality control in smart manufacturing. PhD thesis, Hesam University, Paris, tel-03675240, May.

[28] Q. Li, Y.B. Xu, Z.H. Lai, L.T. Shen, Y.L. Bai, A model of dynamic recrystallisation in alloys during high strain plastic deformation, J. Mater. Sci. Technol. **15** (5), 435-438 (1999).

[29] R.W. Maruda, S. Wojciechowski, N. Szczotkarz, S. Legutko, M. Mia, M.K. Gupta, P. Nieslony, G.M. Krolczyk, Metrological analysis of surface quality aspects in minimum quantity cooling lubrication. Measurement **171**, 108847 (2021).
DOI: https://doi.org/10.1016/j.measurement.2020.108847

[30] Z.K. Ye, Y.L. Wu , G.C. Ma, H. Li, Z.J. Cai, Y.L. Wang, Visual high-precision detection method for tool damage based on visual feature migration and cutting edge reconstruction, Int. J. Adv. Manuf. Technol. **114** (5/6), 1341-1358 (2021).
DOI: https://doi.org/10.1007/s00170-021-06919-5

[31] Z.A.M. Tagiuri, T.M. Dao, A.M. Samuel, V. Songmene, Numerical Prediction of the Performance of Chamfered and Sharp Cutting Tools during Orthogonal Cutting of AISI 1045 Steel, Processes **10** (11), 2171 (2022).
DOI: https://doi.org/10.3390/pr10112171

[32] H. Jirková, K. Rubešová, Š. Jeníček, D. Hradil, L. Kučerová, Improving the Wear Resistance of Ledeburitic Tool Steels by a Combination of Semi-Solid and Cryogenic Processing, Metals **12** (11), 1869 (2022).
DOI: https://doi.org/10.3390/met12111869